



 Cite this: *RSC Adv.*, 2020, 10, 356

# Biocompatible UV-absorbing polymer nanoparticles prepared by electron irradiation for application in sunscreen†

 Sang Yoon Lee, Hyung San Lim, Na Eun Lee and Sung Oh Cho \*

We present a novel approach to preparing non-toxic sunscreen active ingredients by electron irradiation of poly(methyl methacrylate) (PMMA) and polystyrene (PS) nanoparticles (NPs). Electron irradiation modifies the molecular structure of the polymers, generating conjugated aliphatic carbon–carbon double bonds in PMMA and conjugated aromatic rings in PS. The conjugation length increases as the electron fluence increases, leading to hyperchromic and bathochromic shifts in the UV-vis absorption spectra of the irradiated polymer NPs. Consequently, the irradiated polymer NPs become capable of UV absorption and the UV-absorbing properties are improved with increasing electron fluence. The UV-screening performance of the electron-irradiated polymer NPs are found to be superior to those of commercially available sunscreen ingredients. In addition, *in vitro* cytotoxicity and phototoxicity test results show that the irradiated polymer NPs exhibit excellent biocompatibility.

 Received 21st November 2019  
 Accepted 19th December 2019

DOI: 10.1039/c9ra09752j

[rsc.li/rsc-advances](http://rsc.li/rsc-advances)

## Introduction

Overexposure to sunlight may cause detrimental effects, such as increased risk of erythema, photoaging, wrinkling, and even cancer, on the human skin.<sup>1–3</sup> UV radiation present in sunlight can be divided into three subgroups as established in the ISO 21348 standards: UV-A (315–400 nm), UV-B (280–315 nm) and UV-C (100–280 nm).<sup>4</sup> UV-C rays are completely filtered out by the atmosphere, while a fraction of UV-A and UV-B rays reaches the planetary surface.<sup>5</sup> Due to stratospheric ozone depletion, the intensity of UV radiation reaching the surface has increased, and consequently, the rate of skin cancer incidence has risen over the course of the last 50 years.<sup>6,7</sup> In 2018, skin cancer was ranked as the third most commonly occurring cancer worldwide, with it accounting for 7.4% of cancer incidence, which totaled over a million new skin cancer cases within the year.<sup>8</sup> In order to prevent skin cancer and other adverse health effects of UV exposure, sunscreens are widely used. However, there are safety issues regarding the active ingredients in commercially available sunscreens. Sunscreens are composed of organic components, inorganic components or a mixture of both. The organic ingredients, such as avobenzone and octocrylene, are known to cause endocrine disruption and skin irritation.<sup>9,10</sup> Furthermore, these organic compounds are easily decomposed by UV rays, resulting in reduction of their UV-absorbing efficiency over time.<sup>11</sup> The inorganic ingredients, such as titanium

dioxide (TiO<sub>2</sub>) and zinc oxide (ZnO), are generally regarded as being safer than their organic counterparts for their biocompatibility, but they also have drawbacks, such as being opaque and photocatalytic.<sup>12–14</sup> Although inorganic filters have resolved the issue of opaqueness by reducing the particle size to nanoscale, the photocatalytic issue still poses problems when inorganic ingredients are used in sunscreens.<sup>12,15,16</sup> Photocatalytic reactions under UV illumination generate highly reactive oxygen species (ROS) that damage healthy skin cells.<sup>17,18</sup> Thus, to avoid potential harm to individuals resulting from toxicity or phototoxicity of sunscreens, it is necessary to develop non-toxic and photostable UV-absorbing agents.

To overcome the above issues with current sunscreens, various endeavors have been made. Encapsulation methods using safe materials, such as encapsulation of organic UV filters with PMMA or coating of TiO<sub>2</sub> with lignin, have been implemented to reduce the production of ROS.<sup>19,20</sup> Additionally, manganese doped TiO<sub>2</sub> also exhibited reduced ROS generation.<sup>21</sup> Although these approaches have been successful in improving safety by mitigating ROS generation, it is difficult to utilize them practically due to the fact that they cannot guarantee physical stability or uniformity of the modified ingredients.<sup>22</sup> The use of natural plant extract-based ingredients have also been attracting attention in the cosmetic industry, but these ingredients require a convoluted processing procedure and exhibit relatively low quality in terms of UV absorption.<sup>23,24</sup>

Here, we propose a novel route to fabricating non-toxic sunscreen ingredients by electron irradiation of poly(methyl methacrylate) (PMMA) and polystyrene (PS) nanoparticles (NPs). Both polymers are known to be biocompatible and pose no issues concerning biodegradability, bioaccumulation, and

Department of Nuclear and Quantum Engineering, Korea Advanced Institute of Science and Technology, Daejeon, 34141, Republic of Korea. E-mail: socho@kaist.ac.kr

† Electronic supplementary information (ESI) available. See DOI: 10.1039/c9ra09752j



ecotoxicity.<sup>25,26</sup> Due to their biocompatibility, the two polymers are widely used in medical fields as well as in cosmetics as film-forming agents.<sup>25,27,28</sup> In our previous research, we discovered that UV-absorbing property of PS was improved when electron-irradiated.<sup>29</sup> Inspired by this result, we analyzed UV-shielding performance of electron-irradiated PMMA and PS NPs by changing the electron irradiation dose and characterized the cytotoxicity and phototoxicity of the irradiated polymer NPs for potential use in sunscreens.

## Experimental

### Sample preparation

PMMA with an average particle size of 150 nm (SOKEN, Japan) and PS with a diameter of 150 nm (Magsphere, USA) were used in this study. A hundred milligram of NPs were dissolved in 2.5 ml of deionized (DI) water and sonicated for 10 min. The suspension was drop-casted onto a metal plate with a diameter of 8 cm and was then left to dry, forming a film over the plate. Considering that the penetration depth of 50 keV electrons in PMMA and PS are 37.6 and 42.3  $\mu\text{m}$ , respectively, the thickness of the dried polymeric films were prepared to be less than 15  $\mu\text{m}$  to avoid buildup of electrons.

### Electron irradiation

The irradiation procedures were conducted with a thermionic electron gun equipped with a tantalum cathode in a vacuum chamber at a pressure of  $10^{-6}$  torr. The temperature inside the chamber was maintained at  $-5$  °C using a chiller in order to prevent unwanted thermal damage to the samples during irradiation. The energy and the beam current density was set to 50 keV and  $0.5 \mu\text{A cm}^{-2}$ , respectively, and the polymer films were irradiated to various electron fluences with the maximum fluence being  $1.8 \times 10^{17} \text{ cm}^{-2}$ . The electron fluence was controlled by changing the irradiation duration.

### Spectroscopic analyses

UV-vis spectrometer (PerkinElmer, Lambda 1050) fitted with a 150 mm integrating sphere was used in a diffuse reflectance mode to measure optical absorption spectra at the spectral range of 200 to 800 nm. A Fourier-transform infrared (FTIR) spectrometer (Thermo Fisher Scientific Instrument, Nicolet IS50 FTIR) was used in the attenuated total reflection (ATR) mode and a Raman spectrometer (Bruker, RFS 100/S) with a power of 200 mW and an excitation wavelength of 1064 nm were utilized at the wavenumber range of 400 to  $4000 \text{ cm}^{-1}$ .  $^1\text{H}$  NMR (Bruker, Biospin Avance II 900 spectrometer) analysis was performed at a temperature of 20 °C, at a proton resonance frequency of 900 MHz, and at a chemical shift range of 0 to 10 ppm.

### Measurements of UV-screening factors

The polymer NPs were mixed with a non-UV-absorbing sunscreen base and applied to the surface of HD6 plates (Lab-sphere, USA) using a powder-free finger cot. An HD6 plate applied with 15  $\mu\text{l}$  of Vaseline was used as the blank. The treated

plates were allowed to dry for at least 30 min in the dark prior to the measurement process. UV transmittances of the treated plates were measured in the total transmission mode using a UV-vis spectrometer fitted with a 150 mm integrating sphere. The photostability of the polymer NPs was tested using a metal halide UV lamp (Uvitron, UV0834).

## Results and discussion

PMMA and PS are transparent polymers that do not significantly absorb UV rays in their pristine states. However, UV-absorbing properties emerge once the polymers are irradiated with a 50 keV electron beam. The UV-vis absorption spectra show that PMMA and PS NPs absorb significantly more UV rays after electron irradiation; irradiated PMMA and PS exhibit UV (280–400 nm) absorbance values that are 6.9 and 5.1 times the values of their pristine counterparts, respectively (Fig. 1a and b). Images of pristine and electron-irradiated polymer NPs are shown in Fig. S1 (ESI).<sup>†</sup> Additionally, the absorption edges of the irradiated polymers undergo a redshift and their optical bandgaps, the energy difference between the highest occupied molecular orbital (HOMO) and the lowest unoccupied molecular orbital (LUMO), decrease with an increasing electron fluence. Fig. S2 (ESI)<sup>†</sup> shows the optical bandgap of electron-irradiated polymer NPs with respect to electron fluence.

To determine the cause of the UV-absorbing properties of the irradiated polymers and to elucidate the redshift phenomenon, chemical alterations induced by electron irradiation were examined by means of ATR-FTIR, FT-Raman, and  $^1\text{H}$  NMR spectroscopic measurements (Fig. 2). The ATR-FTIR spectra of pristine and irradiated PMMA show that all characteristic peaks of pendant groups, C–H asymmetric stretching at  $2995 \text{ cm}^{-1}$ ,

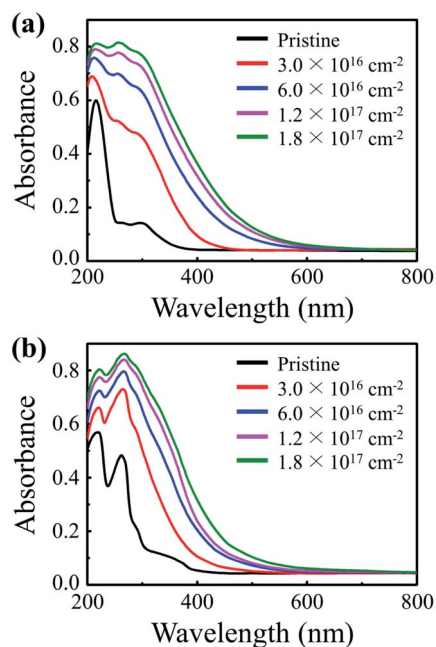


Fig. 1 The UV-vis absorption spectra of (a) PMMA and (b) PS NPs at various electron fluences.



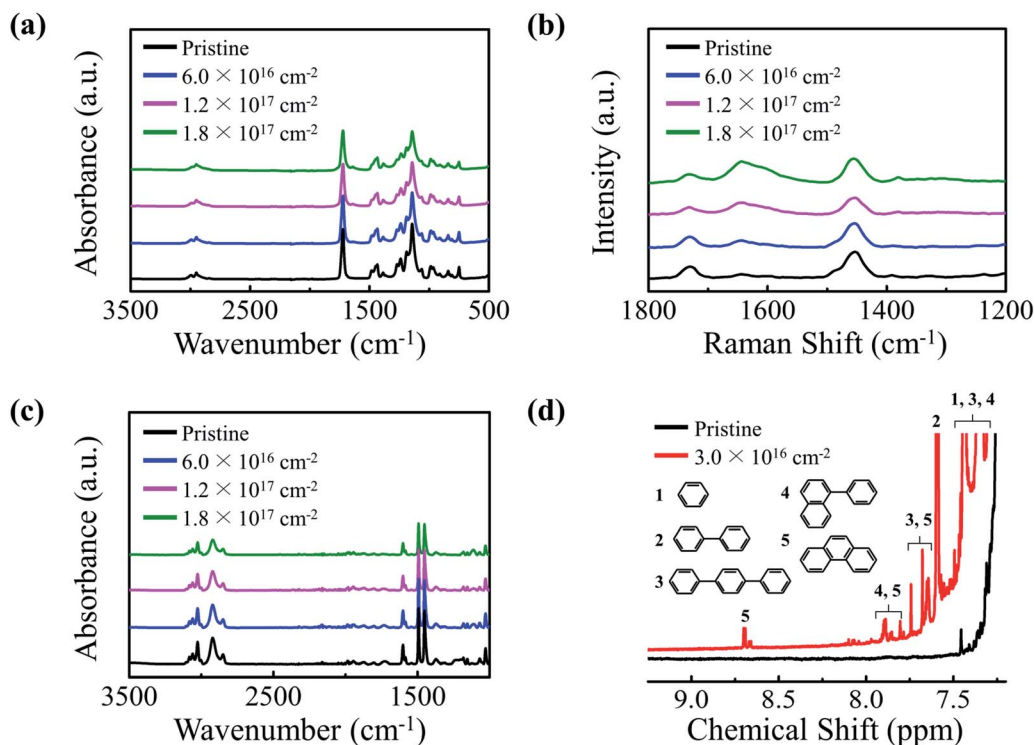


Fig. 2 Spectroscopic results of pristine and electron-irradiated polymers at various electron fluences. (a) ATR-FTIR absorption spectra of PMMA. (b) FT-Raman spectra of PMMA. (c) ATR-FTIR absorption spectra of PS. (d)  $^1\text{H}$  NMR spectra of PS. Inset shows the polycyclic molecules formed by electron irradiation.

$\text{C}=\text{O}$  stretching at  $1722\text{ cm}^{-1}$ ,  $\text{CH}_2$  bending at  $1483\text{ cm}^{-1}$ ,  $\text{C}-\text{O}$  asymmetric stretching at  $1144\text{ cm}^{-1}$ ,  $\text{O}-\text{CH}_3$ -rock at  $987\text{ cm}^{-1}$ ,  $\text{CH}_2$ -rock at  $840\text{ cm}^{-1}$ , and  $\text{C}-\text{C}$  skeletal mode at  $750\text{ cm}^{-1}$  diminish and a new peak at the wavenumber of  $1640\text{ cm}^{-1}$  emerges after electron irradiation (Fig. 2a). The generated peak at  $1640\text{ cm}^{-1}$  indicates the formation of an aliphatic carbon-carbon double bond ( $\text{C}=\text{C}$ ), and this inference is more evidently supported by the Raman measurements (Fig. 2b) and the  $^1\text{H}$  NMR measurements (Fig. S3, ESI $^\dagger$ ). The diminution of FTIR peaks after electron irradiation suggests the occurrence of irradiation-induced chemical bond dissociation, which leads to greater presence of radicals in the polymer. When a pair of radicals are formed from dissociations of two adjacent pendant groups, the unpaired electrons can combine to form a  $\text{C}=\text{C}$  bond at the backbone of PMMA. Extensive electron irradiation can create these  $\text{C}=\text{C}$  bonds at various locations in the polymer, which leads to conjugation of the  $\text{C}=\text{C}$  bonds. The formation mechanism and conjugation process of the  $\text{C}=\text{C}$  bonds are illustrated in Fig. S4 (ESI $^\dagger$ ). Fig. 2c and d show ATR-FTIR and  $^1\text{H}$  NMR measurements that were carried out to determine the cause of the UV-absorbing properties of irradiated PS. The ATR-FTIR results show that the peaks corresponding to aromatic  $\text{C}-\text{H}$  stretching at  $3025\text{ cm}^{-1}$ , aliphatic  $\text{C}-\text{H}$  at  $2917\text{ cm}^{-1}$ , and aromatic  $\text{C}=\text{C}$  stretching at  $1600\text{ cm}^{-1}$  are reduced, indicating that chemical bonds are dissociated by electron irradiation, which leads to formation of various radicals. Raman measurements further support that electron irradiation causes bond dissociation (Fig. S5, ESI $^\dagger$ ). These radicals form conjugated

polycyclic structures through various pathways and the possible pathways are depicted in Fig. S6 (ESI $^\dagger$ ). One such pathway involves electron irradiation causing dissociations of phenyl groups in pristine PS which leads to formation of a reactive phenyl radical, which, when it adheres to another radical formed by dissociation of an aromatic  $\text{C}-\text{H}$  bond, becomes biphenyl. The newly formed resonance peaks in  $^1\text{H}$  NMR spectrum between 7.3 and 8.7 ppm indicate the formation of new molecular structures, which include biphenyl, terphenyl, phenylanthralene, and phenanthrene, resulting from electron irradiation of PS. To encapsulate, conjugated aliphatic  $\text{C}=\text{C}$  bonds are generated in the irradiated PMMA and conjugated polycyclic structures are formed in the irradiated PS. The conjugation lengths of the formed structures in both irradiated PMMA and PS are increased by increasing the electron fluence. As the conjugation length increases, the energy levels of newly formed adjacent  $\pi$  electrons split in accordance with the Pauli exclusion principle, which decreases the energy difference between HOMO and LUMO. This newly generated conjugated system with a lowered optical bandgap allows the absorption of light with longer wavelengths, which elucidates the redshift phenomenon shown in the UV-vis analysis. Thus, the spectral coverage of the irradiated polymers can be controlled by electron fluence, and at the highest electron fluence delivered in this study, the irradiated polymer NPs exhibited significant UV-absorbing properties over a broad UV range.

We investigated the UV-shielding potential of electron-irradiated polymers. Two *in vitro* UV-screening factors, sun



protection factor (SPF) and protection of UVA (PA), were determined following the ISO 24443 guideline. Test samples were prepared by adding the polymer NPs to a non-UV-absorbing test sunscreen base of a DI water and ethanol mixture (a ratio of 6 : 4). The concentration of the polymers in the test samples was fixed at 25%, the maximum allowed concentration of conventional inorganic ingredients in a sunscreen, to allow for comparison of efficacy between the polymer NPs and the inorganic sunscreen ingredients. The prepared test samples were evenly spread over the rough surface of standard HD6 plates until  $1.3 \text{ mg cm}^{-2}$  of the paste was applied. The light transmission rates of the treated plates were then measured using a UV-vis spectrophotometer, and the *in vitro* SPF and PA values were calculated from the following two equations:

$$\text{SPF}_{in vitro} = \frac{\int_{\lambda=290}^{\lambda=400} E(\lambda) \times I(\lambda) \times d\lambda}{\int_{\lambda=290}^{\lambda=400} E(\lambda) \times I(\lambda) \times 10^{-A(\lambda) \times c} \times d\lambda} \quad (1)$$

$$\text{PA}_{in vitro} = \frac{\int_{\lambda=320}^{\lambda=400} P(\lambda) \times I(\lambda) \times d\lambda}{\int_{\lambda=320}^{\lambda=400} P(\lambda) \times I(\lambda) \times 10^{-A(\lambda) \times c} \times d\lambda} \quad (2)$$

where  $E(\lambda)$  is the erythema action spectrum,  $I(\lambda)$  is the spectral irradiance received from the UV source,  $A(\lambda)$  is the mean monochromatic absorbance of the test product layer,  $P(\lambda)$  is the persistent pigment darkening action spectrum,  $c$  is a constant determined from the S2 reference sunscreen formula, and  $d\lambda$  is the wavelength step (1 nm). The SPF and PA values inversely correlate with the mean UV transmission value as the former are determined by factors  $I(\lambda)$ , and  $E(\lambda)$  or  $P(\lambda)$ . Fig. 3a and c shows the SPF and PA values of the test samples containing electron-irradiated PMMA and PS NPs, respectively, as a function of electron fluence. The highest SPF (PA) values obtained for irradiated PMMA and PS were at the highest tested fluence of  $1.8 \times 10^{17} \text{ cm}^{-2}$  with values of 10.2 (6.8) and 13.6 (8.5), respectively. The results show significant promise as the

irradiated polymers outperformed most commonly used sunscreen active ingredients (Table S1, ESI†).

Long-term UV-shielding performance of the irradiated polymer NPs was evaluated by testing their photostability following a guideline provided by the International Conference on Harmonization of Technical Requirements for Registration of Pharmaceuticals for Human Use (ICH).<sup>30</sup> According to studies, it is recommended that sunscreen be reapplied every 2 hours in order to maintain the effectiveness of the sunscreen; thus, preservation of at least 90% of the initial SPF value after two hours of UV illumination is a criterion for determining photostability.<sup>14,31</sup> The irradiated polymer NPs were exposed to UV rays from a sunlight simulating metal halide UV lamp operating at an intensity of  $650 \text{ W m}^{-2}$ , an intensity corresponding to that of global solar spectral irradiance at sea level.<sup>32</sup> Fig. 3b and d shows the SPF values of PMMA and PS NPs irradiated with electrons to a fluence of  $1.8 \times 10^{17} \text{ cm}^{-2}$  as a function of UV exposure time. The results show that extensive UV illumination does not hinder the UV-absorbing properties of the polymer NPs, but rather it slightly enhances the properties, indicating the highly photostable nature of the electron-irradiated polymer NPs.

To evaluate the biocompatibility of the irradiated polymers, both their cytotoxicity and phototoxicity were examined in accordance with the organization for economic cooperation and development (OECD) test guideline (TG) 432 titled *in vitro* 3T3 neutral red uptake phototoxicity test (3T3 NRU PT).<sup>33</sup> Other than

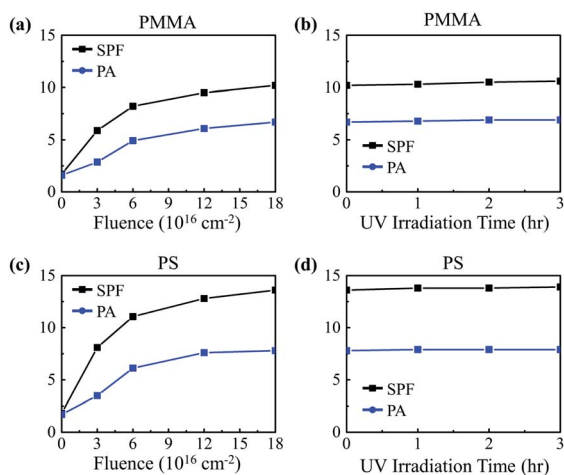


Fig. 3 *In vitro* SPF and PA values of test samples containing pristine and electron-irradiated (a) PMMA and (c) PS NPs as a function of electron fluence. *In vitro* SPF and PA values of the test samples containing electron-irradiated (b) PMMA and (d) PS (electron fluence:  $1.8 \times 10^{17} \text{ cm}^{-2}$ ) as a function of the UV irradiation time.

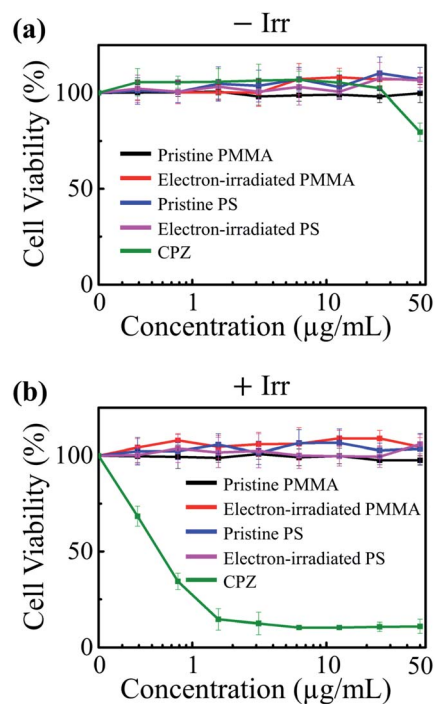


Fig. 4 Cytotoxicity and phototoxicity activities of pristine and electron-irradiated PMMA and PS NPs with the electron fluence of  $1.8 \times 10^{17} \text{ cm}^{-2}$ . Dose-response curves of mean cell viability values in the (a) absence and (b) presence of UVA. Error bars represent standard deviation of six independent measurements.



**Table 1** The phototoxic potential factors and phototoxicity classifications for test substances

Materials	PIF	MPE	Classification
Pristine PMMA	1.0	−0.02	No phototoxicity
Electron-irradiated PMMA	1.0	−0.02	No phototoxicity
Pristine PS	1.0	−0.01	No phototoxicity
Electron-irradiated PS	1.0	−0.05	No phototoxicity
CPZ	48.3	0.32	Phototoxicity

the pristine samples, only those irradiated to the maximum tested fluence of  $1.8 \times 10^{17} \text{ cm}^{-2}$  were examined as they exhibited the most optimal UV-absorbing properties. The cytotoxicity and phototoxicity of the samples were determined by the relative reduction in cell viability of BALB/3T3 cells exposed to irradiated polymers in the absence and presence of UVA illumination (−Irr and +Irr) (Fig. 4a and b). The test samples were exposed to UVA rays (352 nm) with the highest non-cytotoxic dose of  $5 \text{ J m}^{-2}$ . Chlorpromazine (CPZ), a known phototoxic material, was used for positive control. Fig. 4a shows that, under no UV illumination, there were no significant signs of cytotoxicity in the presence of the polymer NPs whether or not the particles were irradiated. To evaluate the phototoxicity of the polymer NPs, we determined the photo irritation factor (PIF) and the mean photo effect (MPE) values following the OECD TG 432. (The details of the guideline are described in the ESI.†) Both phototoxic potential factors have a positive correlation with phototoxicity. The guideline provides the following criteria for phototoxicity classification: substances with a PIF value of less than 2 and an MPE value of less than 0.1 are considered non-phototoxic. The polymer NPs, both irradiated and pristine, exhibit PIF and MPE values less than 2 and 0.1, respectively, indicating no phototoxicity (Table 1). These results demonstrate that the tested polymers are biocompatible even after electron irradiation.

## Conclusions

In conclusion, a novel approach to fabricating non-toxic active ingredients for sunscreens are presented based on electron irradiation of PMMA and PS NPs. Conjugated aliphatic C=C and conjugated aromatic rings are formed in the PMMA and PS, respectively, to produce UV-absorbing traits when the polymers are electron-irradiated. The conjugation length increases with the increase in the electron fluence, leading to a redshift in the absorption spectra. *In vitro* SPF and PA values of the irradiated polymer NPs indicate that the NPs have high photostability as well as highly notable UV-absorbing properties over a broad UV range. The irradiated polymer NPs exhibit no significant signs of cytotoxicity and phototoxicity and are classified as non-phototoxic materials according to OECD TG 432. The electron irradiation technique allows mass production of the nontoxic UV-absorbing NPs. Consequently, the electron irradiation approach provides a good tool to produce non-toxic sunscreen ingredients as alternatives to current sunscreen ingredients that face issues regarding safety. This method can also be applied to

fabrication of photoprotective personal care products, UV-protective textiles, UV-resistant coating, and blue light filters.

## Conflicts of interest

There are no conflicts to declare.

## Acknowledgements

This work was supported by the National Research Foundation of Korea (NRF) grant funded by the Korea government (NRF-2017M2A2A6A02070697).

## References

- 1 F. P. Noonan, J. A. Recio, H. Takayama, P. Duray, M. R. Anver, W. L. Rush, E. C. De Fabo and G. Merlino, *Nature*, 2001, **413**, 271–272.
- 2 H. H. Kim, M. J. Lee, S. R. Lee, K. H. Kim, K. H. Cho, H. C. Eun and J. H. Chung, *Mech. Ageing Dev.*, 2005, **126**, 1170–1177.
- 3 B. K. Armstrong and A. Krieger, *J. Photochem. Photobiol., B*, 2001, **63**, 8–16.
- 4 *Space environment (natural and artificial)—Process for determining solar irradiances, ISO 21348:2007(E)*, 2007.
- 5 D. L. Narayanan, R. N. Saladi and J. L. Fox, *Int. J. Dermatol.*, 2010, **49**, 978–986.
- 6 N. H. Matthews, W.-Q. Li, A. A. Qureshi, M. A. Weinstock and E. Cho, *Epidemiology of melanoma*. Codon Publications, Brisbane, Australia, 2017.
- 7 M. Lin, R. Torbeck, D. Dubin, C. Lin and H. Khorasani, *J. Eur. Acad. Dermatol. Venereol.*, 2019, **33**, e310.
- 8 F. Bray, J. Ferlay, I. Soerjomataram, R. L. Siegel, L. A. Torre and A. Jemal, *Ca-Cancer J. Clin.*, 2018, **68**, 394–424.
- 9 F. H. Yap, H. C. Chua and C. P. Tait, *Australas. J. Dermatol.*, 2017, **58**, e160–e170.
- 10 C. B. Park, J. Jang, S. Kim and Y. J. Kim, *Ecotoxicol. Environ. Saf.*, 2017, **137**, 57–63.
- 11 J. Kockler, M. Oelgemöller, S. Robertson and B. D. Glass, *J. Photochem. Photobiol., C*, 2012, **13**, 91–110.
- 12 M. A. Mitchnick, D. Fairhurst and S. R. Pinnell, *J. Am. Acad. Dermatol.*, 1999, **40**, 85–90.
- 13 H. Shi, R. Magaye, V. Castranova and J. Zhao, *Part. Fibre Toxicol.*, 2013, **10**, 15.
- 14 Y. Tang, F. Wang, C. Jin, H. Liang, X. Zhong and Y. Yang, *Toxicol. Pharmacol.*, 2013, **36**, 66–72.
- 15 T. G. Smijs and S. Pavel, *Nanotechnol., Sci. Appl.*, 2011, **4**, 95–112.
- 16 K. Yu, T. Yoon, A. Minai-Tehrani, J. Kim, S. J. Park, M. S. Jeong, S. Ha, J. Lee, J. S. Kim and M. Cho, *Toxicol. In Vitro*, 2013, **27**, 1187–1195.
- 17 Z.-X. Lu, L. Zhou, Z.-L. Zhang, W.-L. Shi, Z.-X. Xie, H.-Y. Xie, D.-W. Pang and P. Shen, *Langmuir*, 2003, **19**, 8765–8768.
- 18 Y. Guo, V. A. Baulin and F. Thalmann, *Soft Matter*, 2016, **12**, 263–271.
- 19 P.-S. Wu, L.-N. Huang, Y.-C. Guo and C.-C. Lin, *J. Photochem. Photobiol., B*, 2014, **131**, 24–30.



## Paper

- 20 M. Morsella, M. Giammatteo, L. Arrizza, L. Tonucci, M. Bressan and N. d'Alessandro, *RSC Adv.*, 2015, **5**, 57453–57461.
- 21 G. Wakefield, S. Lipscomb, E. Holland and J. Knowland, *Photochem. Photobiol. Sci.*, 2004, **3**, 648–651.
- 22 Y. Wang, R. N. Dave and R. Pfeffer, *J. Supercrit. Fluids*, 2004, **28**, 85–99.
- 23 H. Polonini, M. Brandao and N. Raposo, *RSC Adv.*, 2014, **4**, 62566–62575.
- 24 F. Lohézic-Le Dévéhat, B. Legouin, C. Couteau, J. Boustie and L. Coiffard, *J. Photochem. Photobiol., B*, 2013, **120**, 17–28.
- 25 L. C. Becker, W. F. Bergfeld, D. V. Belsito, R. A. Hill, C. D. Klaassen, D. C. Liebler, J. G. Marks, R. C. Shank, T. J. Slaga and P. W. Snyder, *Internet J. Toxicol.*, 2011, **30**, 54S–65S.
- 26 Y. G. J. Lim, K. C. W. Poh and S. C. J. Loo, *Macromol. Rapid Commun.*, 2019, **40**, 1800801.
- 27 S. R. Cohen, C. F. Berner, M. Busso, P. Clopton, D. Hamilton, J. J. Romano, P. P. Rullan, M. P. Thaler, Z. Ubogy and T. R. Vecchione, *Dermatol. Surg.*, 2007, **33**, S222–S230.
- 28 R. Larsson, G. Selen, H. Björklund and P. Fagerholm, *Biomater*, 1989, **10**, 511–516.
- 29 H. M. Lee, Y. N. Kim, B. H. Kim, S. O. Kim and S. O. Cho, *Adv. Mater.*, 2008, **20**, 2094–2098.
- 30 Stability testing: Photostability testing of new drug substances and products, *ICH, Q1B*, 1996.
- 31 C. Couteau, A. Faure, J. Fortin, E. Papisaris and L. J. Coiffard, *J. Pharm. Biomed. Anal.*, 2007, **44**, 270–273.
- 32 C. Couteau, S. El-Boury, E. Papisaris, V. Sébille-Rivain and L. Coiffard, *Pharm. Dev. Technol.*, 2009, **14**, 369–372.
- 33 *Test No. 432: In Vitro 3T3 NRU Phototoxicity Test*, OECD Publishing, 2004.

